

# Cosmic Ray Acceleration at Relativistic Plasma Flows

MICHAŁ OSTROWSKI

*Obserwatorium Astronomiczne, Uniwersytet Jagielloński, ul. Orła 171, 30-244 Kraków,  
Poland (E-mail: mio@oa.uj.edu.pl)*

**ABSTRACT.** Theoretical concepts of cosmic ray particle acceleration at relativistic plasma flows – shocks and shear layers – are reviewed. We begin with a discussion of mildly relativistic shock waves. The role of oblique field configurations and field perturbations in forming the particle energy spectrum and changing the acceleration time scale is considered. Then, we report on two interesting attempts to consider particle acceleration at ultra-relativistic shocks. Finally, in contrast to the compressive shock discontinuities, we discuss the acceleration processes acting in the boundary layer at the tangential velocity transition. The second-order Fermi acceleration as well as the cosmic ray ‘viscous’ acceleration provide the mechanisms generating energetic particles there.

## 1. Introduction

Relativistic plasma flows are detected or postulated to exist in a number of astrophysical objects, ranging from a mildly relativistic jet of SS433, through the-Lorentz-factor-of-a-few jets in AGNs and galactic ‘mini-quasars’, up to ultra-relativistic outflows in sources of gamma ray bursts and, possibly, in pulsar winds. As nearly all such objects are efficient emitters of synchrotron radiation and/or high energy photons requiring the existence of energetic particles, our attempts to understand the processes generating cosmic ray particles are essential for understanding the fascinating phenomena observed. Below we will discuss the work carried out in order to understand the cosmic ray acceleration processes acting at relativistic flow discontinuities – shocks and shear layers. The present review is an updated version of my earlier presentations (Ostrowski 1996, 1997), also including the discussion of the acceleration at the ultra-relativistic shock by Bednarz & Ostrowski (1998) and the detailed physical model for the pulsar wind terminal shock by Arons and collaborators (cf. Arons 1996).

## 2. Particle acceleration at non-relativistic shock waves

Processes of the first-order particle acceleration at non-relativistic shock waves were widely discussed by a number of authors during the last two decades (for review, see, e.g. Drury 1983, Blandford & Eichler 1987, Berezhko et al. 1988, Jones & Ellison 1991). Below, we review the basic physical picture and some important results obtained within this theory *for test particles*, to be later compared with the results obtained for relativistic shocks.

The simple description of the acceleration process preferred by us consists of considering two plasma rest frames, the *upstream frame* and the *downstream one*. We use indices ‘1’ or ‘2’ to indicate quantities measured in the upstream or the downstream frame respectively. If one neglects the second-order Fermi acceleration, the particle energy is a constant of motion in any of these plasma rest frames and energy changes occur when the particle momentum is Lorentz-transformed at each crossing of the shock. In the case of *parallel* shock, with the mean magnetic field parallel to the shock normal, the acceleration of an individual particle is due to the consecutive shock crossings by the diffusive wandering particle. Each *upstream-downstream-upstream* diffusive loop results in a small increment of particle momentum,  $\Delta p \propto p \cdot (U_1 - U_2)/v$ , where  $v$  is the particle velocity and  $U_i$  is the shock velocity in the respective  $i = 1$  or  $2$  frame,  $U_1 \ll v$ . In oblique shocks, the particle helical trajectories can cross the shock surface a number of times at any individual shock transition or reflection.

The most interesting feature of the first-order Fermi acceleration at a non-relativistic plane-parallel shock wave is the independence of the *test-particle stationary* particle energy spectrum from the background conditions near the shock, including the mean magnetic field configuration and the spectrum of MHD turbulence. The main reason behind that is a nearly-isotropic form of the particle momentum distribution at the shock. If a sufficient amount of scattering occurs near the shock, this condition always holds for the shock velocity along the upstream magnetic field  $U_{B,1} \equiv U_1/\cos\Psi_1 \ll v$  ( $\Psi_1$  - the upstream magnetic field inclination to the shock normal). Independently of the field inclination at the shock, the particle density is continuous across it and the spectral index for the phase-space distribution function,  $\alpha$ , is given exclusively in the terms of a single parameter – the shock compression ratio  $R$ :

$$\alpha = \frac{3R}{R-1} \quad . \quad (2.1)$$

Because of the isotropic form of the particle distribution function, the spatial diffusion equation has become a widely used mathematical tool for describing particle transport and acceleration processes in non-relativistic flows. Thus the characteristic acceleration time scale at the parallel ( $\Psi_1 = 0$ ) shock is

$$T_{acc} = \frac{3}{U_1 - U_2} \left\{ \frac{\kappa_1}{U_1} + \frac{\kappa_2}{U_2} \right\} \quad , \quad (2.2)$$

where  $\kappa_i \equiv \kappa_{\parallel,i}$  is the respective particle spatial diffusion coefficient along the magnetic field, as discussed by e.g. Lagage & Cesarsky (1983). Ostrowski (1988a; see also Bednarz & Ostrowski 1996) derived an analogous expression for shocks with oblique magnetic fields and small amplitude magnetic field perturbations. For a negligible cross-field diffusion and for  $U_{B,1} \ll c$  it can be written in essentially the same form as the one given in Eq. (2.2), with all quantities taken as the normal ( $n$ ) ones with respect to the shock ( $\kappa_{n,i}$  for  $\kappa_i$  ( $i = 1, 2$ )). As  $\kappa_n < \kappa_{\parallel}$ , the oblique shocks may be more rapid accelerators when compared to the parallel shocks.

Not discussed here non-linear and time dependent effects, inclusion of additional energy losses and gains, etc., make the physics of the acceleration more intricate, allowing e.g. for non-power-law and/or non-stationary particle distributions.

### 3. Cosmic ray acceleration at relativistic shock waves

#### 3.1. The Fokker-Planck description of the acceleration process

In the case of the shock velocity (or its projection  $U_{B,1}$ ) reaching values comparable to the light velocity, the particle distribution at the shock becomes anisotropic. This fact complicates to a great extent both the physical picture and the mathematical description of particle acceleration. The first attempt to consider the acceleration process at the relativistic shock was presented in 1981 by Peacock (see also Webb 1985); however, no consistent theory was proposed until a paper of Kirk & Schneider (1987a; see also Kirk 1988) appeared. Those authors considered the stationary solutions of the relativistic Fokker-Planck equation for particle pitch-angle diffusion for the case of the parallel shock wave. In the situation with the gyro-phase averaged distribution  $f(p, \mu, z)$ , which depends only on the unique spatial co-ordinate  $z$  along the shock velocity, and with  $\mu$  being the pitch-angle cosine, the equation takes the form:

$$\Gamma(U + v\mu) \frac{\partial f}{\partial z} = C(f) + S \quad , \quad (3.1)$$

where  $\Gamma \equiv 1/\sqrt{1-U^2}$  is the flow Lorentz factor,  $C(f)$  is the collision operator and  $S$  is the source function. In the presented approach, the spatial co-ordinates are measured in the shock rest frame, while the particle momentum co-ordinates and the collision operator are given in the respective plasma rest frame. For the applied pitch-angle diffusion operator,  $C = \partial/\partial\mu(D_{\mu\mu}\partial f/\partial\mu)$ , they generalised the diffusive approach to higher order terms in particle distribution anisotropy and constructed general solutions at both sides of the shock which involved solutions of the eigenvalue problem. By matching two solutions at the shock, the spectral index of the resulting power-law particle distribution can be found by taking into account a sufficiently large number of eigenfunctions. The same procedure yields the particle angular distribution and the spatial density distribution. The low-order truncation in this approach corresponds to the standard diffusion approximation and to a somewhat more general method described by Peacock. The above analytic approach (or the ‘semi-analytic’ one, as the mentioned matching of two series involves numerical fitting of the respective coefficients) was verified by Kirk & Schneider (1987b) by the method of particle Monte Carlo simulations.

An application of this approach to more realistic conditions – but still for parallel shocks – was presented by Heavens & Drury (1988), who investigated the fluid dynamics of relativistic shocks (cf. also Ellison & Reynolds 1991) and used the results to calculate spectral indices for accelerated particles (Fig. 1). They considered the shock wave propagating into electron-proton or electron-positron plasma, and performed calculations using the analytic method of Kirk & Schneider for two different power spectra for the scattering MHD waves. In contrast to the non-relativistic case, they found (see also Kirk 1988) that the particle spectral index depends on the form of the wave spectrum. The unexpected fact was noted that the non-relativistic expression (2.1) provided a quite reasonable approximation to the actual spectral index.

A substantial progress in understanding the acceleration process in the presence of highly anisotropic particle distributions is due to the work of Kirk & Heavens (1989;

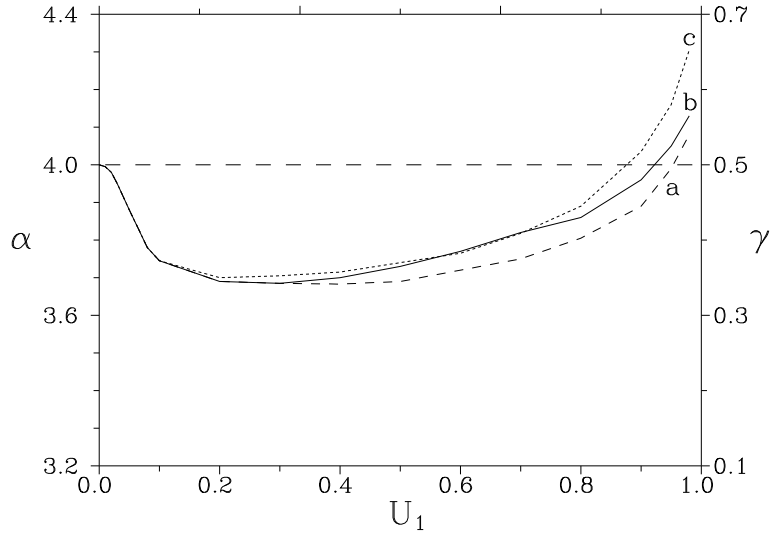


Fig. 1. The particle spectral indices  $\alpha$  at parallel shock waves propagating in the cold ( $e, p$ ) plasma versus the shock velocity  $U_1$  (Heavens & Drury 1988). On the right vertical axis the respective synchrotron spectral index  $\gamma$  is given. Using the solid line (b) and the dashed line (a) we show indices for two choices of the turbulence spectrum. The dashed line (c) gives the spectral index derived from Eq. 2.1. The horizontal line  $\alpha = 4.0$  is given for the reference.

see also Ostrowski 1991a and Ballard & Heavens 1991), who considered particle acceleration at *subluminal* ( $U_{B,1} < c$ ) relativistic shocks with oblique magnetic fields. They assumed the magnetic momentum conservation,  $p_{\perp}^2/B = \text{const}$ , at particle interaction with the shock and applied the Fokker-Planck equation discussed above to describe particle transport along the field lines outside the shock, while excluding the possibility of cross-field diffusion. In the cases when  $U_{B,1}$  reached relativistic values, they derived very flat energy spectra with  $\gamma \approx 0$  at  $U_{B,1} \approx 1$  (Fig. 2). In such conditions, the particle density in front of the shock can substantially – even by a few orders of magnitude – exceed the downstream density (see the curve denoted ‘-8.9’ at Fig. 3). Creating flat spectra and great density contrasts is due to the effective reflections of anisotropically distributed upstream particles from the region of compressed magnetic field downstream of the shock. However, the conditions leading to very flat spectra are supposed to be accompanied by processes – like a large amplitude wave generation upstream of the shock – leading to spectrum steepening (cf. Sec. 3.2).

As stressed by Begelman & Kirk (1990), in relativistic shocks one can often find the *superluminal* conditions with  $U_{B,1} > c$ , where the above presented approach is no longer valid. Then, it is not possible to reflect upstream particles from the shock and to transmit downstream particles into the upstream region. In effect, only a single transmission of upstream particles re-shapes the original distribution by shifting particle energies to larger values. The energy gains in such a process, involving a highly anisotropic particle distribution, can be quite significant, exceeding the value expected for the adiabatic

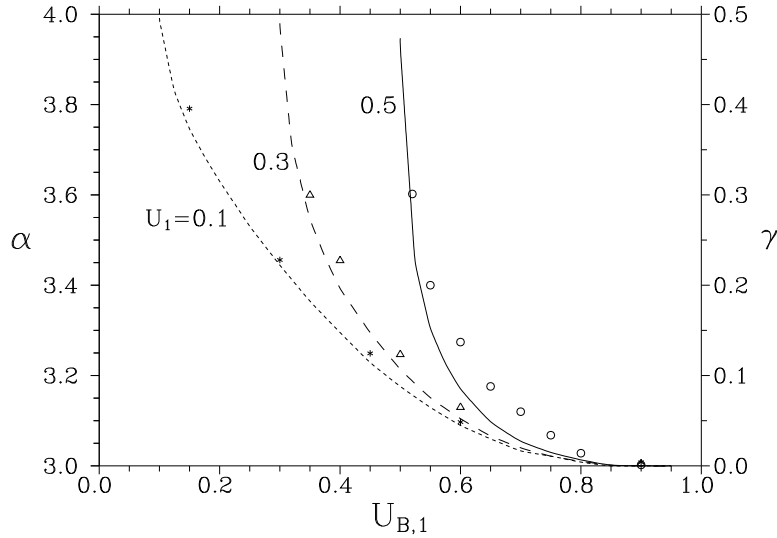


Fig. 2. Spectral indices  $\alpha$  of particles accelerated at oblique shocks versus shock velocity projected at the mean magnetic field,  $U_{B,1}$ . On the right the respective synchrotron spectral index  $\gamma$  is given. The shock velocities  $U_1$  are given near the respective curves taken from Kirk & Heavens (1989). The points were taken from simulations deriving explicitly the details of particle-shock interactions (Ostrowski 1991a). The results are presented for compression  $R = 4$ .

compression.

The approach proposed by Kirk & Schneider (1987a) and Kirk & Heavens (1989), and the derivations of Begelman & Kirk (1990) are valid only in case of weakly perturbed magnetic fields. However, in the efficiently accelerating shocks one may expect large amplitude waves to be present, when both the Fokker-Planck approach is no longer valid and the magnetic momentum conservation no longer holds for oblique shocks. In such a case, numerical methods have to be used.

### 3.2. Particle acceleration in the presence of large amplitude magnetic field perturbations

The first attempt to consider the acceleration process at parallel shock wave propagating in a turbulent medium was presented by Kirk & Schneider (1988), who included into Eq. 3.1 the Boltzmann collision operator describing the large angle scattering. By solving the resulting integro-differential equation they demonstrated the hardening of the particle spectrum due to increasing contribution of the large-angle scattering. The reason for such a spectral change is the additional isotropization of particles interacting with the shock, leading to an increase in the particle mean energy gain. In oblique shocks, this simplified approach cannot be used because the character of individual particle-shock interaction – reflection and transmission characteristics – depends on the magnetic field perturbations. Let us additionally note that application of the point-like large-angle scattering model in relativistic shocks does not provide a viable physical representation of the scattering at MHD waves (Bednarz & Ostrowski 1996).

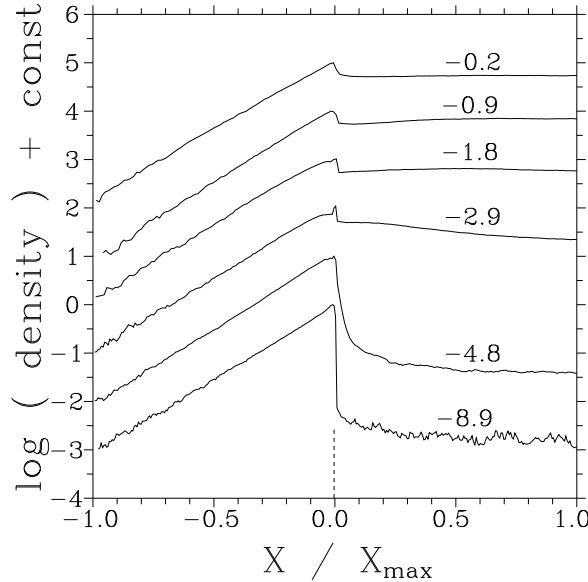


Fig. 3. The energetic particle density across the relativistic shock with an oblique magnetic field (Ostrowski 1991b). The shock with  $U_1 = 0.5$ ,  $R = 5.11$  and  $\psi_1 = 55^\circ$  is considered. The curves for different perturbation amplitudes are characterized with the value  $\log \kappa_\perp / \kappa_\parallel$  given near the curve. The data are vertically shifted for picture clarity. The value  $X_{max}$  is the distance from the shock at which the upstream particle density decreases to  $10^{-3}$  part of the shock value.

To handle the problem of the particle spectrum in a wide range of background conditions, the Monte Carlo particle simulations were proposed (Kirk & Schneider 1987b; Ellison et al. 1990; Ostrowski 1991a, 1993; Ballard & Heavens 1992, Naito & Takahara 1995, Bednarz & Ostrowski 1996, 1998). At first, let us consider subluminal shocks. The field perturbations influence the acceleration process in various ways. As they enable the particle cross field diffusion, a modification (decrease) of the downstream particle's escape probability may occur. This factor tends to harden the spectrum. Next, the perturbations decrease particle anisotropy, leading to an increase of the mean energy gain of reflected upstream particles, but – what is more important for oblique shocks – this also increases the particle upstream-downstream transmission probability due to less efficient reflections, enabling them to escape from further acceleration. The third factor is due to perturbing particle trajectory during an individual interaction with the shock discontinuity and breakdown of the approximate conservation of  $p_\perp^2 / B$ . Because reflecting a particle from the shock requires a fine tuning of the particle trajectory with respect to the shock surface, even small amplitude perturbations can decrease the reflection probability in a substantial way. Simulations show (see Fig. 4 for  $U_{B,1} < 1.0$ ) that – until the wave amplitude becomes very large – the factors leading to efficient particle escape dominate with the resulting steepening of the spectrum to  $\gamma \sim 0.5 - 0.8$ , and the increased downstream transmission probability lowers the cosmic ray density contrast

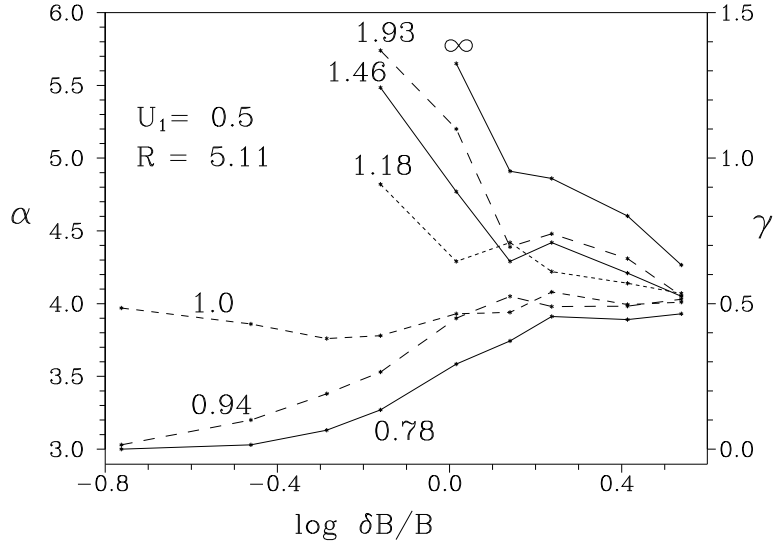


Fig. 4. Spectral indices for oblique relativistic shocks versus perturbation amplitude  $\delta B/B$  (Ostrowski 1993). Different field inclinations are characterized by the values of  $U_{B,1}$  given near the respective results,  $U_{B,1} < 1$  for subluminal shocks and  $U_{B,1} \geq 1$  for superluminal ones. Absence of data for small field amplitudes in superluminal shocks is due to extremely steep power law spectra occurring in these conditions (cf. Begelman & Kirk 1990). Decreasing the field inclination  $\Psi_1 \rightarrow 0$  (i.e to the parallel shock with  $U_{B,1} = U_1$ ) gives spectral indices more and more similar to a constant line  $\alpha = 3.72$ , not shown here for picture clarity (cf. Fig-s 1,2).

across the shock (Fig. 3).

In parallel shock waves propagating in a highly turbulent medium, the effects discovered for oblique shocks can also manifest their presence because of the *local* perturbed magnetic field compression at the shock. The problem was considered using the technique of particle simulations by Ballard & Heavens (1992; cf. Ostrowski 1988b for non-relativistic shock). They showed a possibility of having a very steep spectrum in this case, with the spectral index growing from  $\gamma \sim 0.6$  at medium relativistic velocities up to nearly 2.0 at  $U_1 = 0.98$ . These results apparently do not correspond to the large-perturbation-amplitude limit of Ostrowski's (1993; see the discussion therein) simulations for oblique shocks and the analytic results of Heavens & Drury (1988).

For large amplitude magnetic field perturbations the acceleration process in superluminal shocks can lead to the power-law particle spectrum formation, against the statements of Begelman & Kirk (1990) valid at small wave amplitudes only. Such a general case was discussed by Ostrowski (1993; see Fig. 4 for  $U_{B,1} \geq 1$ ) and by Bednarz & Ostrowski (1996, 1998).

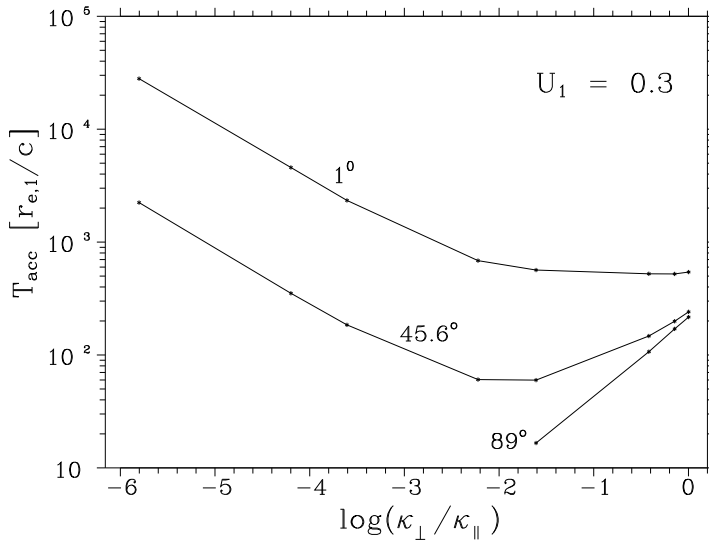


Fig. 5. The acceleration time  $T_{acc}$  versus the level of particle scattering measured by the ratio of  $\kappa_{\perp}/\kappa_{\parallel}$  ( Bednarz & Ostrowski 1996). We present results for three values of the magnetic field inclination: a.) parallel shock ( $\psi_1 = 1^\circ$ ), b.) a subluminal shock with  $\psi_1 = 45.6^\circ$  and c.) a superluminal shock with  $\psi_1 = 89^\circ$ .  $r_{e,1}$  is the particle gyroradius in the effective (including perturbations) upstream magnetic field .

### 3.3. The acceleration time scale

The shock waves propagating with relativistic velocities also raise interesting questions pertaining to the cosmic ray acceleration time scale,  $T_{acc}$ . A simple comparison to non-relativistic values shows that  $T_{acc}$  relatively decreases with increasing shock velocity for parallel (Quenby & Lieu 1989; Ellison et al. 1990) and oblique (Takahara & Terasawa 1990; Newman et al. 1992; Lieu et al. 1994; Quenby & Drolias 1995; Naito & Takahara 1995) shocks. However, the numerical approaches used there, based on assuming particle isotropization for all scatterings, neglect or underestimate a significant factor affecting the acceleration process – the particle anisotropy. Ellison et al. (1990) and Naito & Takahara (1995) also included the more realistic, in our opinion, derivations involving the pitch-angle diffusion approach. The calculations of Ellison et al. for parallel shocks show similar results to those they obtained for large amplitude scattering. For the shock with velocity  $0.98 c$  the acceleration time scale is reduced by the factor  $\sim 3$  with respect to the non-relativistic formula of Eq. 2.2 . Naito & Takahara considered shocks with oblique magnetic fields. They confirmed the reduction of the acceleration time scale with an increasing inclination of the magnetic field, derived earlier for non-relativistic shocks. However, their approach neglected effects of particle cross field diffusion and assumed the adiabatic invariant conservation in particle interactions with the shock, thus limiting the validity of their results to a small amplitude turbulence near the shock.

A wider discussion of the acceleration time scale is presented by Bednarz & Ostrowski

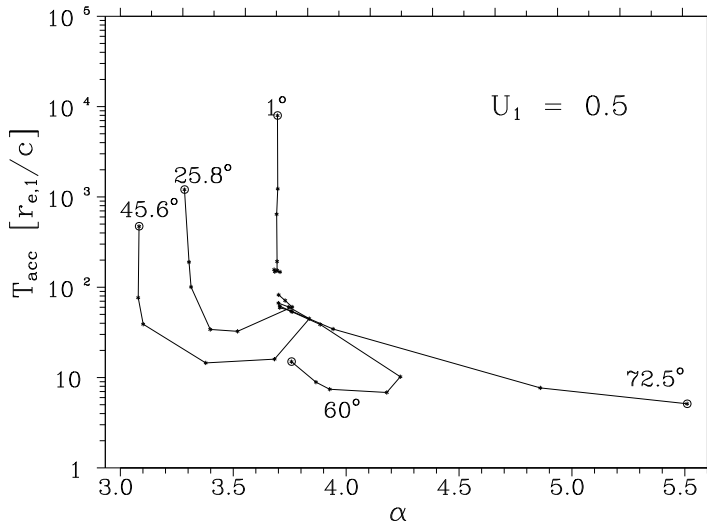


Fig. 6. The relation of  $T_{acc}$  versus the particle spectral index  $\alpha$  at different magnetic field inclinations  $\psi_1$  given near the respective curves. The *minimum* value of the model parameter  $\kappa_{\perp}/\kappa_{\parallel}$  occurs at the encircled point of each curve and the wave amplitude monotonously increases along each curve up to  $\delta B \sim B$ ;  $r_{e,1}$  – see Fig. 5.

(1996), who apply numerical simulations involving the small angle particle momentum scattering. The approach is also believed to provide a reasonable description of particle transport in the presence of large  $\delta B$ , and thus to enable modelling of the effects of cross-field diffusion. The resulting values (Figs 5, 6) are given in the shock *normal* rest frame (cf. Begelman & Kirk 1990). In parallel ( $\Psi_1 = 1^\circ$ ) shocks  $T_{acc}$  diminishes with the growing perturbation amplitude and shock velocity  $U_1$ . However, it is approximately constant for a given value of  $U_1$  if we use the formal diffusive time scale,  $\kappa_1/(U_1 c) + \kappa_2/(U_2 c)$ , as the time unit. A new feature discovered in oblique shocks is that due to the cross-field diffusion  $T_{acc}$  can change with  $\delta B$  in a non-monotonic way (Fig. 5). The acceleration process leading to the power-law spectrum is possible in superluminal shocks only in the presence of large amplitude turbulence. Then, in contrast to the quasi-parallel shocks,  $T_{acc}$  increases with increasing  $\delta B$ . In the considered cases with the oblique field configurations one may note a possibility to have an extremely short acceleration time scale comparable to the particle gyroperiod in the magnetic field upstream of the shock. A coupling between the acceleration time scale and the particle spectral index is presented in Fig. 6. One should note that the form of involved relation is contingent to a great extent on the magnetic field configuration.

### 3.4. Energy spectra of cosmic rays accelerated at large Lorentz-factor shocks

The main difficulty in modelling the acceleration process at shocks with large Lorentz factors  $\Gamma$  is the fact that the involved particle distributions are extremely anisotropic in

the shock, with the particle angular distribution opening angles  $\sim \Gamma^{-1}$  in the upstream plasma rest frame. When transmitted downstream of the shock, particles have a limited chance to be scattered so efficiently as to reach the shock again, but the energy gain of any such ‘successful’ particle can be comparable to, but not much larger than its original energy<sup>1</sup>. In the simulations of Bednarz & Ostrowski (1998) a hybrid Monte Carlo method involving small amplitude pitch-angle scattering is applied for particle transport near the shock with  $\Gamma$  in the range 3 – 243. The same scattering conditions upstream and downstream of the shock (the same  $\kappa_{\perp}$  and  $\kappa_{\parallel}$  in the units of  $r_g c$ , where  $r_g$  is the particle gyration radius in the unperturbed background magnetic field) were assumed. A few configurations of the upstream magnetic field, with inclinations respective to the shock normal being  $\psi = 0^\circ, 10^\circ, 20^\circ, 30^\circ, 60^\circ$  and  $90^\circ$  were considered. The first case represents the parallel shock, the second is for the oblique – subluminal at  $\Gamma = 3$  and superluminal at larger  $\Gamma$  – shock, and the larger  $\psi$  are for superluminal perpendicular shocks at all velocities. The downstream magnetic field is derived for the relativistic shock with the compression  $R$  obtained with the formulae of Heavens and Drury (1988) for a cold ( $e, p$ ) plasma (however, at so high  $\Gamma$  it weakly depends on this particular choice).

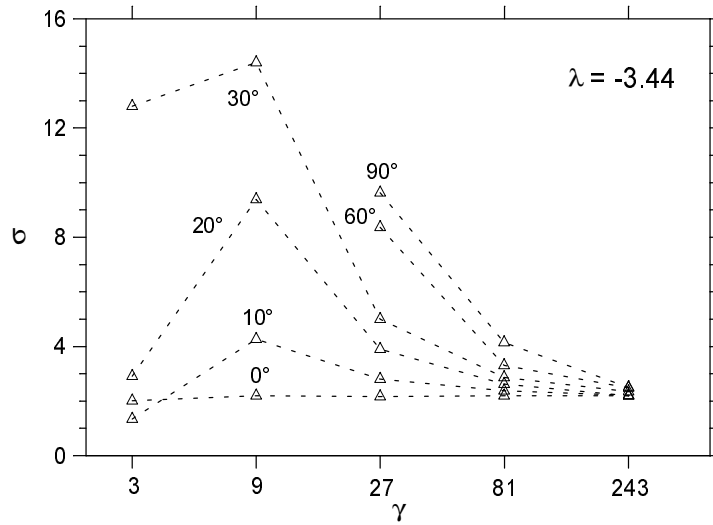


Fig. 7. The simulated spectral indices  $\sigma$  ( $\sigma \equiv \alpha - 2$ ) versus  $\Gamma$ . Results for a given  $\psi$  are joined with dashed lines; the respective value of  $\psi$  is given near each curve. Increasing of parameter  $\lambda$  results in shifting curves toward the stable  $\Psi = 0^\circ$  results.

Results for varying  $\psi$  at some intermediate  $\lambda \equiv \kappa_{\perp}/\kappa_{\parallel}$  are presented at Fig. 7. For the parallel shock ( $\psi = 0^\circ$ ) the amount of scattering does not influence the spectral index and for growing  $\Gamma$  it approaches  $\sigma_{\infty} \simeq 2.2$ . Essentially the same limiting value

<sup>1</sup> It is impossible to reflect a charged particle from the large- $\Gamma$  shock if a magnetic field is present upstream of it. The shock will always overtake the upstream escaping particle. The reflections with relative energy gains  $\sim \Gamma^2$  are in principle possible from the sides of jets (see below).

was anticipated for the large- $\Gamma$  parallel shocks by Heavens and Drury (1988). The results for  $\psi = 10^\circ$  are for superluminal shocks if  $\Gamma > 5.75$ . In this case, when going from the ‘slow’  $\Gamma = 3$  shocks to the higher  $\Gamma$  ones, at first the spectrum inclination increases ( $\sigma$  grows), but at large  $\Gamma$  the spectrum flattens to approach the asymptotic value close to 2.2. The spectrum steepening phase – usually interpreted as an energy cut-off – is more pronounced for small  $\kappa_\perp/\kappa_\parallel$ , but even at very low turbulence levels the final range of spectrum flattening is observed. For larger  $\psi$  the situation does not change, but the phase of spectrum steepening is wider, involves larger values of  $\sigma$  and starts at smaller velocities. In the case of large spectral indices occurring in the steepening phase the main factor increasing the particle energy density is a non-adiabatic compression in the shock (Begelman & Kirk 1990).

The inspection of particle trajectories reveals a simple picture of acceleration. Cosmic ray particles are wandering in the downstream region with the shock wave moving away with the mildly relativistic velocity  $\approx c/3$ . Some of these particles succeed to reach the shock, but then they remain in the upstream region for a very short time – being very close to the shock – due to large shock velocity  $\approx c$ . This scenario is essentially equivalent to the picture involving downstream particles reflecting in a non-elastic way from the receding wall of the shock. For large- $\Gamma$  shocks any particle crossing the shock upstream has a momentum vector nearly parallel to the shock normal, the momentum inclination must be smaller than  $\theta_{max} = \arccos(U_1) \ll 1$ . If the scattering or a movement along the curved trajectory increases this inclination above  $\theta_{max}$  the particle tends to re-cross the shock downstream. One should note that even a tiny – comparable to  $\theta_{max}$  – angular deviation in the upstream plasma ( $\Delta\theta_U$ ) can lead to large angular deviation for  $\Gamma \gg 1$  as observed in the downstream rest frame. The phenomenon of decreasing  $\sigma$  to  $\sigma_\infty$  at constant  $\lambda$  and for growing  $\Gamma$  results from slower diminishing of the part of  $\Delta\theta_U$  caused by scattering in comparison to the one arising due to trajectory curvature in the uniform field component<sup>2</sup>. As a result the particles crossing the shock downstream are scattered in a wide angular range with respect to the shock normal, providing some particles with parameters allowing for re-crossing upstream of the shock even for the perpendicular magnetic field configuration. An interesting finding, not fully explained with such simple arguments is the fact that the number of such particles re-crossing the shock becomes nearly independent of the magnetic field inclination and the turbulence amplitude. It is also observed that when approaching the limiting value of the spectral index the mean particle energy gain  $\langle \Delta E/E \rangle$  in the cycle ‘upstream-downstream-upstream’ reaches a value close (slightly above) to 1.0, much smaller than the factor  $\sim \Gamma^2$  expected for a model involving large angle point-like scattering.

### 3.5. Acceleration at the ultra-relativistic shock near the Crab Pulsar

As discussed above, the details of the acceleration process can substantially modify particle spectra in relativistic shocks. Thus the knowledge of some details of the shock transition deserves the effort to make the model more specific. Such an approach was presented by Arons and collaborators (e.g. Hoshino et al. 1992, Gallant & Arons 1994; for

---

<sup>2</sup> This way the magnetic field structure defined by  $\psi$  becomes unimportant. One should also note that the downstream field inclination approaches  $90^\circ$  if  $\psi \neq 0$  and  $\Gamma \rightarrow \infty$ .

review Arons 1996), who considered acceleration at the ultra-relativistic shock formed in the wind outflow of the ( $e^+, e^-$ ) pair plasma containing heavy nuclei and being permeated by the weak magnetic field oriented perpendicular to the flow direction, i.e. in a model wind for the Crab Pulsar. In the large Lorentz factor wind, the ram pressure of nuclei dominates over the ram pressure of the pair plasma, and both these pressures are much larger than the magnetic field pressure.

At the collisionless shock, the pairs' bulk velocity is isotropized much more efficiently, leaving nuclei penetrating the downstream region as a particle beam. This process generates an electric field in the shock and – due to the ion distribution anisotropy – generates long electromagnetic plasma waves. Damping of such waves by pairs accelerates some of electrons/positrons to energies allowing for the creation of the observed TeV photons and synchrotron radiation up to several tens of MeV. In this model, gyroradii of nuclei are comparable to the radial size of the shock ( $\approx 0.1$  pc) and this component is suspected to be responsible for optical wisps observed in the Crab (Gallant & Arons 1994). The work mentioned here is based on the results of numerical plasma simulations of the ultra-relativistic collisionless shock. If this approach points into the right physics, then the presented work could be evaluated as the only realistic model of the acceleration process for relativistic shocks available in literature.

#### 4. Energetic particle acceleration at a relativistic shear layer

There is a list of observations pointing to the fact that acceleration processes acting e.g. in AGNs central sources and in shocks formed in jets are not always able to explain the observed high energy electrons radiating away from the centre/shock. Among a few proposed possibilities explaining these data the relatively natural but unexplored is the one involving particle acceleration at a tangential velocity ‘jump’ or a shear layer at the interface between the jet and the surrounding medium (‘cocoon’). To date the knowledge of physical conditions within such layers is very limited and only rough estimates for the considered acceleration processes are possible. Within the *subsonic* turbulent layer with a non-vanishing small velocity shear the ordinary second-order Fermi acceleration, as well as the process of ‘viscous’ particle acceleration (cf. the review by Berezhko (1990) of the work done in early 80-th; also Earl et al. 1988, Ostrowski 1990, 1998) can take place. A mean particle energy gain in the later process scales as

$$\langle \Delta E \rangle \propto \left( \frac{\langle \Delta U \rangle}{c} \right)^2, \quad (4.1)$$

where  $\langle \Delta U \rangle$  is the mean velocity difference between the ‘successive scattering acts’. It is proportional to the mean free path normal to the shear layer,  $\lambda_n$ , times the mean flow velocity gradient in this direction  $\nabla_n \cdot \mathbf{U}$ . With  $d$  denoting the shear layer thickness this gradient can be estimated as  $|\nabla_n \cdot \mathbf{U}| \approx U/d$ . Because the acceleration rate in the Fermi II process is  $\propto (V/c)^2$  ( $V \approx V_A$  is the wave velocity,  $V_A$  – the Alfvén velocity), the relative importance of both processes is given by a factor

$$\left( \frac{\lambda_n U}{d V} \right)^2. \quad (4.2)$$

The relative efficiency of the viscous acceleration grows with  $\lambda_n$  and in the formal limit of  $\lambda_n \approx d$  – outside the equation (4.2) validity range – it dominates over the Fermi acceleration to a large extent. Because accelerated particles can escape from the accelerating layer only due to a relatively inefficient radial diffusion, the resulting particle spectra should be very flat up to the high energy cut-off, but the exact form of the spectrum depends on several unknown physical parameters of the boundary layer. More solid information can be obtained about generated spectra of ‘*very high*’ energy particles, where a particle belongs to this class if  $\lambda_n \geq d$  (or  $r_g > d$ ). A few results for such particles accelerated in the absence of radiation losses are presented below.

#### 4.1. Acceleration of very high energy particles: terminal shock versus the jet’s side boundary

For sufficiently energetic particles both the jet terminal shock and the transition layer between the jet and the surrounding medium can be approximated as surfaces of discontinuous velocity change. The later tangential discontinuity can be an efficient cosmic ray acceleration site if the considered velocity difference is relativistic and the sufficient amount of turbulence on its both sides is present (Berezhko 1990, Ostrowski 1990). On average, at a single boundary crossing a particle gains

$$\langle \Delta E \rangle = \rho_e (\Gamma - 1) E_0 \quad , \quad (4.3)$$

where  $\Gamma$  is the jet Lorentz factor and the numerical factor  $\rho_e$  depends on the particles anisotropy at the discontinuity. Particle simulations described by Ostrowski (1990), in the presence of efficient particle scattering, give  $\rho_e$  as a substantial fraction of unity. Let us also note that in the case of a non-relativistic velocity jump,  $U \ll c$ , the acceleration process is of the second-order in  $U/c$ .

Spectra of particles accelerated at relativistic shock waves depend in a large extent on the poorly known physical conditions near the shock. Therefore, instead of attempting to reproduce a detailed shape of the particle spectrum let us, rather, consider a modification introduced to the *power-law with a cut-off* shock spectrum by the additional acceleration at the jet boundary (Ostrowski 1998). We neglect the radiation losses, i.e. the upper energy limit is fixed by the boundary conditions – the finite shock and jet spatial extensions – allowing for the escape of the highest energy particles. Let us consider the jet terminal shock resting with respect to the cocoon surrounding the jet. The conditions occurring behind the shock due to the flow divergence are modelled by imposing the particle free escape boundary at a finite distance,  $L_{esc}$ , downstream of the shock and in the cocoon adjoining this boundary. Also, another tube-like free escape boundary is introduced, surrounding the jet in a distance  $R_{esc}$  from the jet axis. We assume the mean magnetic field to be parallel to the jet velocity both within the jet and in the cocoon. Possible significant deviations from this simple structure are partly accommodated in the simulations by also considering cases with unrealistically large cross-field diffusion. In the presented examples we take a ratio  $D$  of the cross-field diffusion coefficient to the parallel diffusion coefficient to be 0.0013 or 0.97.

In Fig. 8 one can consider spectra of particles escaping through the boundaries for the seed particle injection far upstream of the terminal shock and – for  $U_1 = 0.5$  –

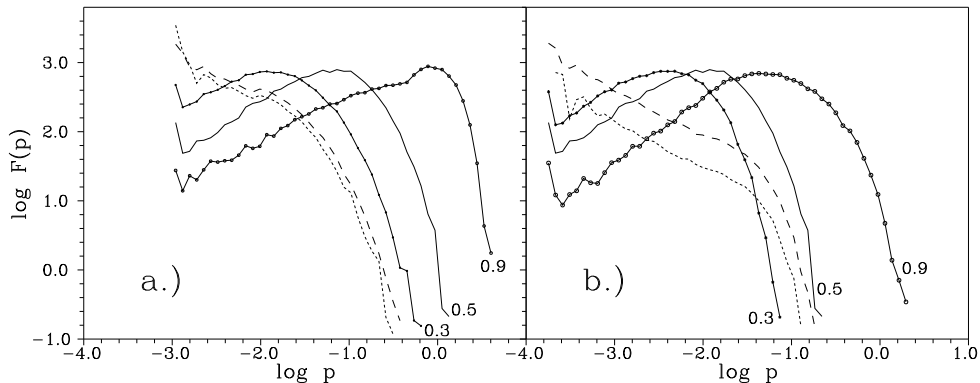


Fig. 8. Simulated particle distributions  $F(p) \equiv dN(p)/d(\log p)$ . Particles with the momentum  $p = 1.0$  have a gyroradius equal to the jet radius,  $R_j$  and the injection momentum is  $p_0 \ll 1$ . We take  $R_{esc} = 2R_j$  and  $L_{esc} = R_j$ . Full lines represent the spectra for particles injected at the distance of  $1000R_j$  upstream of the terminal shock; the respective jet velocities  $U_1$  are given near these lines. The curve with long dashes denotes the spectrum for the terminal shock injection, while the one with shorter dashes presents the spectrum for the upstream injection with the side boundary acceleration neglected (these curves are for  $U_1 = 0.5$ ). At the left panel (a) the results for the smaller cross-field diffusion  $D = 0.0013$  are presented, while in the right panel (b) results for the nearly isotropic diffusion  $D = 0.97$  are given.

compare these spectra to the ones generated at the shock. One may note that the distribution of particles accelerated at the jet side-boundary is very flat. This feature results from the character of the acceleration process with particles having a chance to meet the accelerating surface again and again due to inefficient diffusive escape to the sides. Contrary to that, the shock acceleration process determines the spectrum inclination due to the joint action of the particle energization at the shock and the continuous escape due to particle advection with the plasma. In the present simulations fixed spatial distances to the escape boundaries are assumed. Thus the escape probability grows with the particle momentum providing an energy cut-off in the spectrum. For the shock spectrum (Fig. 8b), in the range of particle energies directly preceding the cut-off, the spectrum exhibits some flattening with respect to the inclination expected for the standard shock acceleration mechanism. There are two reasons for that flattening: additional particle transport from the downstream shock region to the upstream one through the cocoon surrounding the jet and inclusion of the very flat spectral component resulting from the side boundary acceleration.

#### 4.2. Large Lorentz factor jets

The expected in close vicinity of AGNs highly relativistic jets provide an exceptionally promising sites for accelerating particles. The only requirement is that some sufficiently energetic, with  $\lambda_n \sim d$ , seed particles exist in the jet vicinity. As even single interactions

of such particles with the jet may boost its' energies on large factors (cf. Eq. 4.3), a rapid build-up of the cosmic ray energy density may result, with the bulk of energy contained in highest energy particles. If these particles become dynamically important one could speculate about the intermittent behaviour of the generated cosmic ray population providing the time modulation of the jet structure and the produced high energy photon field.

#### 4.3. Shear layers near the black hole accretion disks

The same mechanism can work in all conditions allowing for large velocity gradients. One such suggested possibility arises in the vicinity of the accretion disk near the accreting black hole. A recent work of Subramanian et al. (1998) proposed this process to provide the energy source for ejection of the high Lorentz factor jets from vicinity of the quasar central engine.

### 5. Final remarks

The work done to date on the *test particle* cosmic ray acceleration at mildly relativistic shocks yielded not too promising results for meaningful modelling of the observed astrophysical sources. The main reason for that deficiency is – in contrast to non-relativistic shocks – a direct dependence of the derived spectra on the conditions at the shock. Not only the shock compression ratio, but also other parameters, like the mean inclination of the magnetic field or the wave spectrum shape and amplitude, are significant here. Depending on the actual conditions one may obtain spectral indices as flat as  $\alpha = 3.0$  ( $\gamma = 0.0$ ) or very steep ones with  $\alpha > 5.0$  ( $\gamma > 1.0$ ). The background conditions leading to the very flat spectra are probably subject to some instabilities; however, there is no detailed derivation describing the instability growth and the resulting cosmic ray spectrum modification. The situation may become simpler for large  $\Gamma$  shocks, where – in the simulations of Bednarz & Ostrowski (1998) – the spectral index converges to the universal limit  $\sigma_\infty \approx 2.2$ .

A true progress in modelling particle acceleration in actual sources requires a full plasma non-linear description, including feedback of accelerated particles at the turbulent wave fields near the shock wave, flow modification caused by the cosmic rays' plasma pre-shock compression and, of course, the appropriate boundary conditions. A simple approach to the parallel shock case was presented by Baring & Kirk (1990), who found that relativistic shocks could be very efficient accelerators. However, it seems to us that in a more general case it will be very difficult to make any substantial progress in that matter. For very flat particle spectra the non-linear acceleration picture depends to a large extent on the detailed knowledge of the background and boundary conditions in the scales relevant for particles near the upper energy cut-off. The existence of stationary solutions is doubtful in this case. An important step toward considering detailed physics of the acceleration provides the work of Arons and collaborators described in Section 3.5, applicable in ultra-relativistic shocks.

One may note that observations of possible sites of relativistic shock waves (knots and hot spots in extragalactic radio sources), which allow for the determination of the

energetic electron spectra, often yield particle spectral indices close to  $\alpha = 4.0$  ( $\gamma = 0.5$ ). In order to overcome difficulties in accounting for these data Ostrowski (1994) proposed an additional ‘*law of nature*’ for non-linear cosmic ray accelerators. The particles within different energy ranges do not couple directly with each other and are supposed to form independent ‘degrees of freedom’ in the system. Our ‘law’ provides that nature prefers energy equipartition between such degrees of freedom, yielding the spectra with  $\alpha \approx 4.0$ .

The acceleration processes at astrophysical shear layers may provide a viable explanation for some ‘strange’ observational data. For example it may have significant consequences for the relativistic jet structure, particularly on the sub-parsec scales, and on the high energy photon radiation fields of AGNs (Ostrowski, in preparation). Also, these mechanisms could be responsible for accelerating particles up to the ultra high energies above EeV scales (Ostrowski 1998). An application of the viscous acceleration for the shear layer near the accretion disc in the AGN centre was presented by Subramanian et al. (1998). The discussed processes are particularly interesting because a simple inspection does not reveal any physical obstacles which could make them inefficient. Unfortunately, the resulting electron spectra depend to a large extent on the poorly known background physical conditions.

### Acknowledgements

The present work was supported by the *Komitet Badań Naukowych* through the grant PB 179/P03/96/11.

### References

- Arons J., 1996, *Astron. Astrophys. Suppl. Ser.* **120**, 49  
Ballard, K.R., Heavens, A.F., 1991, *Mon. Not. R. Astr. Soc.* **251**, 438  
Ballard, K.R., Heavens, A.F., 1992, *Mon. Not. R. Astr. Soc.* **259**, 89  
Baring, M.G., Kirk, J.G., 1990, *Astron. Astrophys.* **241**, 329  
Bednarz J., Ostrowski M., 1996, *Mon. Not. R. Astr. Soc.* **283**, 447  
Bednarz J., Ostrowski M., 1998, *Phys. Rev. Lett.* **80**, 3911  
Begelman, M.C., Kirk J.G., 1990, *Astrophys. J.* **353**, 66  
Berezhko, E.G., 1990, Preprint ‘*Frictional Acceleration of Cosmic Rays*’, The Yakut Scientific Centre, Yakutsk  
Berezhko, E.G., Iolshin, W.K., Krymskij, G.F., Pietukhov, S.I., 1988, *Cosmic Ray Generation at Shock Waves* (in Russian), Nauka, Moscow.  
Blandford, R.D., Eichler, D., 1987, *Physics Reports* **154**, 1  
Drury, L.O’C., 1983, *Rep. Prog. Phys.* **46**, 973  
Earl J.A., Jokipii J.R., Morfill G., 1988, *Astrophys. J.* **331**, L91  
Ellison, D.C., Jones, F.C., Reynolds, S.P., 1990, *Astrophys. J.* **360**, 702  
Ellison, D.C., Reynolds, S.P., 1991, *Astrophys. J.* **382**, 242  
Gallant Y.A., Arons J., 1994, *Astrophys. J.* **435**, 230  
Heavens, A., Drury, L’O.C., 1988, *Mon. Not. R. Astr. Soc.* **235**, 997  
Hoshino M., Arons J., Gallant Y.A., Langdon A.B., 1992, *Astrophys. J.* **390**, 454  
Jones, F.C., Ellison, D.C., 1991, *Space Sci. Rev.* **58**, 259

- Kirk J.G., 1988, *Habilitation Theses*, preprint No. 345, Max-Planck-Institut für Astrophysik, Garching
- Kirk J.G., 1997, in Proc. Int. Conf. *Relativistic Jets in AGNs*, eds. M. Ostrowski, M. Sikora, G. Madejski, M. Begelman; Cracow (p. 145)
- Kirk, J.G., Heavens, A., 1989, *Mon. Not. R. Astr. Soc.* **239**, 995
- Kirk, J.G., Schneider, P., 1987a, *Astrophys. J.* **315**, 425
- Kirk, J.G., Schneider, P., 1987b, *Astrophys. J.* **322**, 256
- Kirk J.G., Schneider P., 1988, *Astron. Astrophys.* **201**, 177
- Lagage P.O., Cesarsky C., 1983, *Astron. Astrophys.* **125**, 249
- Lieu, R., Quenby, J.J., Drolias, B., Naidu, K., 1994, *Astrophys. J.* **421**, 211
- Naito T., Takahara F., 1995, *Mon. Not. R. Astr. Soc.* **275**, 1077
- Newman P.L., Moussas X., Quenby J.J., Valdes-Galicia J.F., Theodossiou-Ekaterinidi Z., 1992, *Astron. Astrophys.* **255**, 443
- Ostrowski, M., 1988a, *Mon. Not. R. Astr. Soc.* **233**, 257
- Ostrowski, M., 1988b, *Astron. Astrophys.* **206**, 169
- Ostrowski, M., 1990, *Astron. Astrophys.* **238**, 435
- Ostrowski, M., 1991a, *Mon. Not. R. Astr. Soc.* **249**, 551
- Ostrowski, M., 1991b, in ‘*Relativistic Hadrons in Cosmic Compact Objects*’, eds. A. Zdziarski and M. Sikora (p. 121)
- Ostrowski, M., 1993, *Mon. Not. R. Astr. Soc.* **264**, 248
- Ostrowski, M., 1994, *Comments on Astrophysics* **17**, 207
- Ostrowski, M., 1996, in Proc. Int. Symp. on *Extremely High Energy Cosmic Rays*, ed. M. Nagano, Tanashi (p. 68)
- Ostrowski M., 1997, in Proc. Int. Conf. ‘*Relativistic Jets in AGNs*’, eds. M. Ostrowski, M. Sikora, G. Madejski, M. Begelman; Cracow (p. 153)
- Ostrowski M., 1998, *Astron. Astrophys.* **335**, 134
- Peacock, J.A., 1981, *Mon. Not. R. Astr. Soc.* **196**, 135
- Quenby J.J., Lieu R., 1989, *Nature* **342**, 654
- Quenby J.J., Drolias B., 1995, in Proc. 24th Int. Cosmic Ray Conf., 3, 261, Rome
- Subramanian P., Becker P.A., Kazanas D., 1998, preprint astro-ph/9805044
- Takahara F., Terasawa T., 1990, in Proc. ICRR Int. Symp. ‘*Astrophysical Aspects of the Most Energetic Cosmic Rays*’, eds. M. Nagano & F. Takahara, Kofu
- Webb, G.M., 1985. *Astrophys. J.* **296**, 319